



**Volume 23 (2016)**

**Supporting information for article:**

**Vanadium *K*-edge XANES in vanadium-bearing model compounds: a full multiple scattering study**

**Federico Benzi, Gabriele Giuli, Stefano Della Longa and Eleonora Paris**

# V K-edge XANES in V-bearing model compounds: a Full Multiple Scattering study. Supplementary information

F. Benzi, G. Giuli, S. della Longa and E. Paris

## 1 Calculation details for palenzonaite

From the crystallographic data the atomic cluster is built, centered around a V atom. Since the FMS theory does not allow partial occupation of the sites we simplified the palenzonaite structure in  $\text{Ca}_3\text{Mn}_2(\text{VO}_4)_3$ , *i.e.* by filling all of the dodecahedral sites with Ca, all of the Octahedral sites with Mn and all of the tetrahedral sites with V. We checked the convergence of the theoretical calculations with the size of the cluster, and with  $lmax$ , which is the angular momentum cutoff for the spherical harmonics expansion in the calculation of the FMS equation. First, we performed XANES simulations increasing the cluster size by including further V coordination shells (Fig. 1). We started by calculating a theoretical spectrum using only 5 scatterers (the central V and the 4 oxygen atoms in the tetrahedron, (Fig. 1 lower spectrum)). Further coordination shells are then added to the starting cluster. For example, in the second spectrum (19 atoms) we added a Ca and Mn shell. At around 51 atoms all of the features are roughly reproduced, but only after including 90 atoms in the cluster we reached convergence. Then we performed similar calculations by fixing the number of scatterers to 90 and varying the value of  $lmax$  (Fig. 2). Increasing too much this number can cause drastic performance reduction of the calculation.

As a general behaviour the value of  $lmax$  follows the rule of “the higher the better”, but it is possible to find a good compromise between the accuracy and the speed of the calculation. As it can be seen in Fig. 2 the calculation differs significantly between  $lmax = 2$  and  $lmax = 3$  (the relative peak intensities and peak positions are significantly different). On the other hand calculations performed at  $lmax = 3$  and  $lmax = 4$  show similar relative peak intensities and position, so we decided to use  $lmax = 3$  as the standard value for the fit.

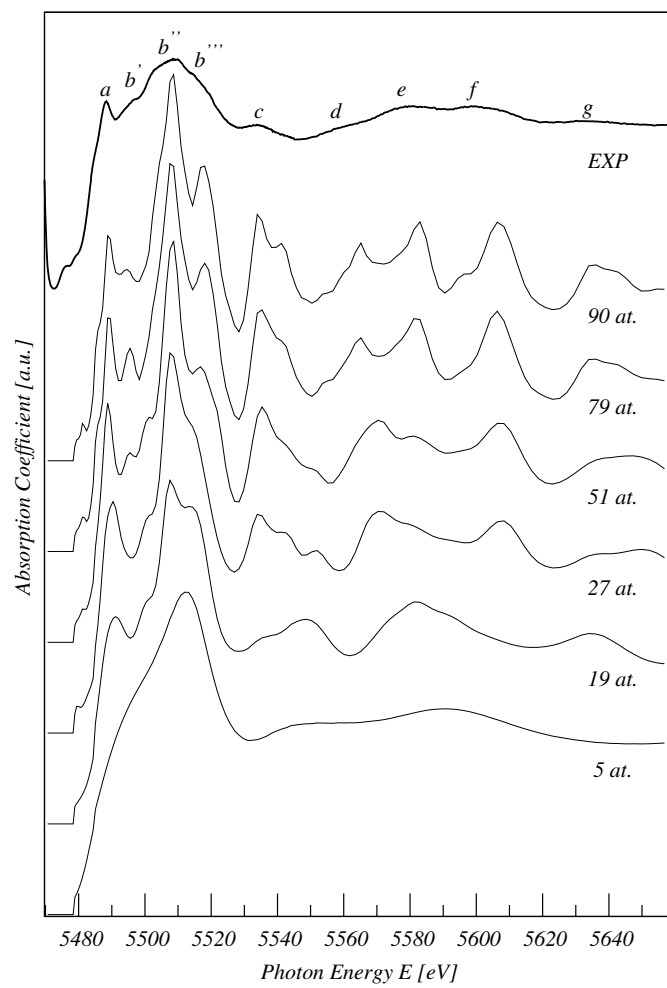


Figure 1: Palenzonaite MXAN calculations performed increasing the number of scattering atoms. The experimental spectrum is drawn on top.

Another way to assess the limits for the cluster size and the angular momentum cutoff can be derived by calculating the absolute difference between two consecutive spectra. In case of palenzonaite it was clear to choose the number of scatterers: the difference between the spectra calculated with 5 and 19 scatterers and 19 and 27 scatterers was in the order of 0.35, while dropping to around 0.25 for the next two calculations and finally to 0.1 when adding 90 atoms. At the same time the difference between  $lmax = 2$  and 3 was in the order of 0.4, while the difference between  $lmax = 3$  and 4 was again 0.1.

Since in our model the T site is fully occupied by V, instead of a combination of V, As and Si we decided to optimize the size of the first shell. Starting from a theoretical value of 1.714 Å we let the 4 V-O distances of the first shell to change coherently of about 5%. So the MS fit parameters were the MT overlap (*ovlp*), the interstitial potential ( $V0_{imp}$ ) and the radius of the first shell (R1); the alignment parameters were an energy shift (*ensh*), a normalization factor (*norm*) and a factor to account for the residual slope of the experimental spectrum (*slope*); finally the broadening parameters were the core hole lifetime (fixed to the theoretical value of 1.01, *broad*), the experimental resolution (*broad exp*), the plasmon onset energy (*epl*) and the plasmon intensity (*apl*). Since the RSMS theory may not be accurate for the calculation of the transitions to the bound states (the pre-edge peak), we decided to add a  $\Theta$ -like function weight to the fit, whose onset starts at -2 eV with respect to  $E_0$ .

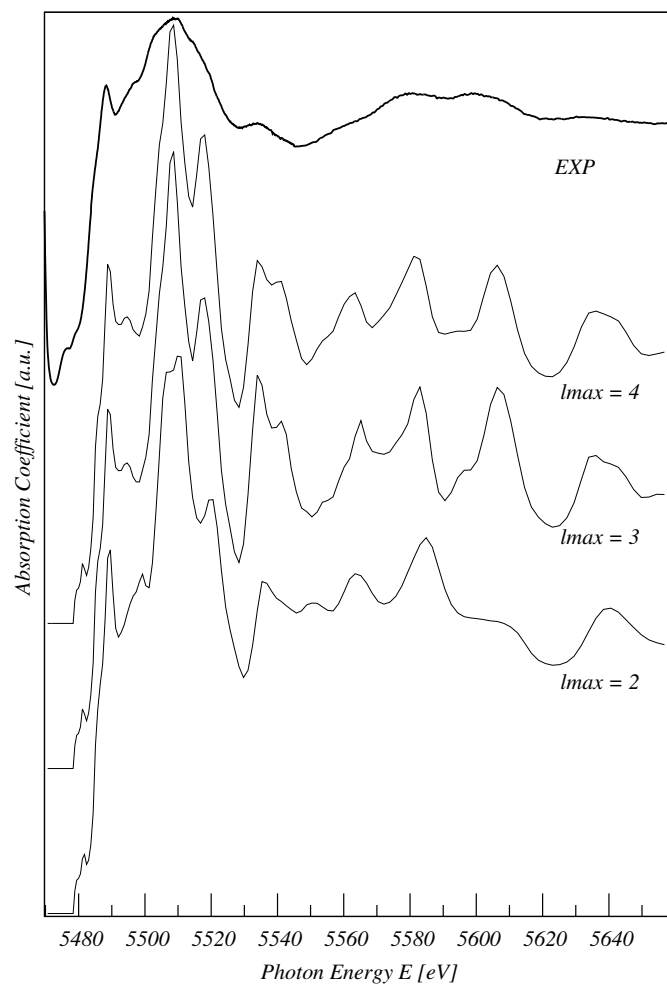


Figure 2: Palenzonaite MXAN calculations performed increasing  $l_{max}$ . The experimental spectrum is represented on top.

## 2 Fit details for all model compounds

Structural data and MT parameters			
V-O ( $\text{\AA}$ )		1.689(2)	
ovlp		0.202(1)	
V0inp (eV)		-12.5(8)	
sq.res.		3.9	
nscs		90	
lmax		3	
Alignment and broadening parameters			
ensh (eV)	5478.9	norm	0.039
fermi (eV)	-2.82	Broad (eV)	1.0+0.5
Epl (eV)	12.12	Apl	11.16
Muffin-tin radii ( $\text{\AA}$ )			
	V		1.090
	O		0.945
	Na		1.810

Table 1: Palenzonaite fit results. The number in brackets represents the error on the last digit. No error is available for broadening and alignment parameters since they have been calculated using the Monte-carlo method. The two values for the broad parameters refer to the core-hole lifetime (fixed for simplicity to 1 eV instead of the theoretical value of 1.01 eV, since there is no difference in the calculated spectra) and the experimental resolution. The value of sq.res. represents the sum of the square of the residual and gives an indication of the goodness of the fit.

Structure and MT parameters			
V-O ( $\text{\AA}$ )	2.03	(1)	
ovlp	0.078	(5)	
V0inp (eV)	-9.3	(6)	
sq.res.	9.5		
nsca	123		
lmax	3		
Alignment and broadening parameters			
ensh (eV)	5478.86	norm	0.043
fermi (eV)	-2.76	Broad (eV)	1.0+0.5
Epl (eV)	20.2	Apl	12.2
Muffin-tin radii ( $\text{\AA}$ )			
V	1.248		
O <sub>1</sub>	0.821		
O <sub>2</sub>	0.827		
Ca	1.554		

Table 2: Goldmanite fit results. The number in brackets represents the error on the last digit. No error is available for broadening and alignment parameters since they have been calculated using the Monte-carlo method. The two values for the broad parameters refer to the core-hole lifetime (fixed to the theoretical value of 1) and the experimental resolution.

Structure and MT parameters			
$V - O_1$ (Å)		1.62(2)	
$V - O_2$ (Å)		2.00(2)	
$V - O_3$ (Å)		2.02(2)	
ovlp		0.27(2)	
V0inp (eV)		-9.9(7)	
sq.res.		1.6	

Alignment and broadening parameters			
ensh (eV)	5478.6	norm	0.044
fermi (eV)	-4.2	Broad (eV)	1.0+0.5
Epl (eV)	22.0	Apl	18.1

Muffin-tin radii (Å)	
V	1.149
O <sub>1</sub>	0.919
O <sub>2</sub>	0.961
O <sub>2</sub>	0.951
Wat	1.847
Si	1.085

Table 3: Cavansite fit results. The number in brackets represents the error on the last digit. No error is available for broadening and alignment parameters since they have been calculated using the Monte-carlo method. The two values for the broad parameters refer to the core-hole lifetime (fixed to the theoretical value of 1) and the experimental resolution.



Structure and MT parameters			
$V - O_1$ (Å)		1.68(1)	
$V - O_2$ (Å)		1.68(2)	
$V - O_3$ (Å)		1.68(5)	
ovlp		0.21(4)	
V0inp (eV)		-13.8(8)	
sq.res.		1.9	
nscs		90	
lmax		4	
Alignment and broadening parameters			
ensh (eV)	5476.1	norm	0.040
fermi (eV)	-3.2	Broad (eV)	1.0+0.5
Epl (eV)	15.5	Apl	17.0
Muffin-tin radii (Å)			
V		1.096	
O <sub>1</sub>		0.957	
O <sub>2</sub>		0.962	
O <sub>3</sub>		0.976	
Pb <sub>1</sub>		1.755	
Pb <sub>2</sub>		1.794	

Table 4: Vanadinite fit results. The number in brackets represents the error on the last digit. No error is available for broadening and alignment parameters since they have been calculated using the Monte-carlo method. The two values for the broad parameters refer to the core-hole lifetime (fixed to the theoretical value of 1) and the experimental resolution.

Structure and MT parameters			
ovlp		0.07	(1)
V0inp (eV)		-14.0	(6)
sq.res.		10.7	
nsca		110	
lmax		4	
Alignment and broadening parameters			
ensh (eV)	5479.6	norm	0.044
fermi (eV)	-4.7	Broad (eV)	1.0+0.8
Epl (eV)	22.2	Apl	24.8
Muffin-tin radii (Å)			
	V	1.196	
	O	0.921	

Table 5:  $V_2O_3$  fit results. The number in brackets represents the error on the last digit. No error is available for broadening and alignment parameters since they have been calculated using the Monte-carlo method. The two values for the broad parameters refer to the core-hole lifetime (fixed to the theoretical value of 1) and the experimental resolution.

Structure and MT parameters			
ovlp		0.14	(1)
V0inp (eV)		-17.0	(2)
sq.res.		10.6	
nsca		102	
lmax		4	
Alignment and broadening parameters			
ensh (eV)	5479.03	norm	0.042
fermi (eV)	-2.87	Broad (eV)	1.0+0.5
Epl (eV)	14.7	Apl	10.5
Muffin-tin radii ( $\text{\AA}$ )			
	V	1.091	
	O <sub>1</sub>	0.919	
	O <sub>2</sub>	0.874	

Table 6:  $V_2O_4$  fit results. The number in brackets represents the error on the last digit. No error is available for broadening and alignment parameters since they have been calculated using the Monte-carlo method. The two values for the broad parameters refer to the core-hole lifetime (fixed to the theoretical value of 1) and the experimental resolution.

Structure and MT parameters			
ovlp		0.28(2)	
V0inp (eV)		-12.3(8)	
sq.res.		3.4	
nsca		119	
lmax		4	
Alignment and broadening parameters			
ensh (eV)	5478.22	norm	0.043
fermi (eV)	-3.0	Broad (eV)	1.0+0.5
Epl (eV)	12.56	Apl	10.3
Muffin-tin radii ( $\text{\AA}$ )			
	V		1.105
	O <sub>1</sub>		0.921
	O <sub>2</sub>		1.047
	O <sub>3</sub>		1.0091

Table 7:  $V_2O_5$  fit results. The number in brackets represents the error on the last digit. No error is available for broadening and alignment parameters since they have been calculated using the Monte-carlo method. The two values for the broad parameters refer to the core-hole lifetime (fixed to the theoretical value of 1) and the experimental resolution.